Development of 3-dimensional Imaging System for the Full-field Imaging Soft X-ray Microscope at BL-12

Takuji Ohigashi[1], Hiroki Fujii[2], Kishin Usui[2], Hidetoshi Namba[2], Kuniko Takemoto[3] and Hiroshi Kihara[3]

Abstract

The optical system of the full-field imaging soft x-ray microscope at BL-12 was modified for 3-dimensional observation by using computer tomography. A new sample stage set including the high precision rotational stage was installed. Smaller head parts for the condenser optics were designed to obtain clearance between the sample and the head parts. A larger pinhole (diameter of 20 μm) was used for obtaining deeper focal depth of ~12 μm and for more photon flux instead of the degradation of the spatial resolution. Furthermore, for stabilization of the environment, the housing for the optical system was built to prevent airflow from the outside and to decrease the temperature fluctuation. The temperature fluctuation was decreased down from 9.1×10^{-3} to 5.3×10^{-4} [°C/min]. By using this system, the 3-dimensional structures of a test sample, an extended glass capillary tube and polystyrene spheres, and iron bacterium were observed.

---

[1] *Research Organization of Science & Engineering, Ritsumeikan University, 1-1-1 Noji Higashi, Kusatsu, Shiga, Japan*

[2] *Department of Physics, Ritsumeikan University, 1-1-1 Noji Higashi, Kusatsu, Shiga, Japan*

[3] *Department of Physics, Kansai Medical University, 18-89 Uyamahigashi, Hirakata, Osaka, Japan*

1. Introduction

3-dimensional observation is an expected technique for the structural study. The computer tomography (CT) is the promising method for the 3-dimensional observation without any destructive processes and is one of the remarkable advantages of the x-ray imaging. This method brings 3-dimensional internal structures as maps of linear absorption coefficients by reconstructing 2-dimensional x-ray transmission images. Since the size of the sample which the soft x-ray can penetrate is compatible with the spatial resolution of the soft x-ray microscope, the CT method is suitable well for combination with the soft x-ray microscope. The sample of several micron can be observed 3-dimensionally with several tens nano meter order resolution. Thus the CT by using the soft x-ray microscope has been realized widely [1-4].

The full-field imaging soft x-ray microscope (SXRM) at BL-12 was designed to observe biological samples by using the wavelength of the water window region [5, 6]. For performing the CT by using this system, some problems should be solved. New hardware, a rational stage for the sample, is required but the installation of the rotational axis of the sample to the SXRM is not so easy for very small space around the sample. The parameters, especially the focal depth and the stability, need to be optimized. The focal depth is the most important parameter for the imaging CT. As for the stability, acquisition of one CT dataset takes long time generally, more than a few hours in our case so that long-term stability of the optical system (e.g. accuracy of the rotational axis of the sample, low thermal drift, no airflow and so on) is highly required. Since the BL-12 is placed in front of the entrance of the experimental hall, its environment, such as temperature, airflow and noise from passer-by, is not stable at all. These factors should be improved for better performance.

In this study, modification of the optical system, improvements of the environment are discussed and some results of the 3-dimensional observation are shown.

2. Modification of optical system

For performing the CT, the concept of the optical system differs from that of the 2-D imaging. The sample for the CT may be relatively thicker than that of the 2-D imaging and should be wholly placed within the focal depth of the SXRM. Then, we must decide whether observation of the small sample or lengthening the focal depth. The latter one was selected so the optical parameters of the SXRM were modified. In parallel, the sample stage set and hardware were changed.

At diffraction limit imaging at the wavelength of 2.3 nm, the calculated focal depth is 3.23 μm. This focal depth is too narrow so that the wavelength resolution of the condenser optics was degraded for using the deeper focal depth. Then, the spatial resolution would be also degraded for the cromatic aberration of the FZP. The wavelength resolution, $\lambda/\Delta\lambda$, of the linear monochromator which consists of a pinhole and the condenser FZP is defined by

$$\lambda / \Delta\lambda = D / 2d \qquad (1)$$

where D is diameter of the condenser FZP and d is diameter of pinhole [7]. For the SXRM at BL-12, the pinhole of ϕ15 μm is used as usual and the wavelength resolution of 300 is obtained. In this study, the pinhole of ϕ 20 μm was used and the wavelength resolution was degraded to 225. The practical focal depth and the spatial resolution of the SXRM were evaluated experimentally. By observing the horizontal edge of a Ni #150 mesh with the wavelength of 2.3 nm, the edge response (20 ~ 80%) was plotted against the position of the objective FZP in Fig. 1. Length of flat part at the bottom of the fitted curve, at the edge response of about 120 nm, the practical focal depth of about 12 μm was obtained. This focal depth is regarded as moderate length for performing the CT by considering transmittance of water (~30%) and the size of field of view (ϕ ~10 μm) at the wavelength of 2.3 nm.

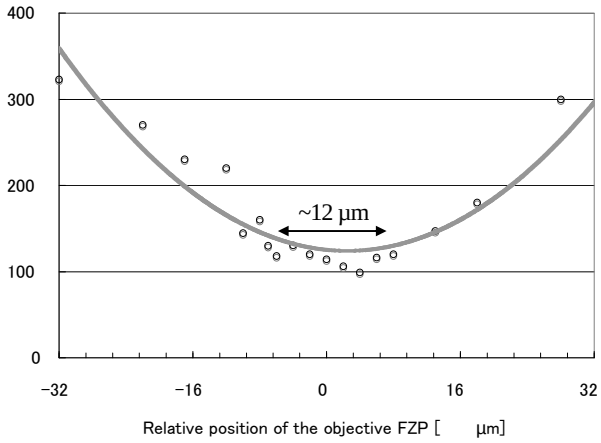

Fig. 1: Focal depth evaluated from edge response

A new head part for the condenser optics was designed. The diameter of the new head part is about half the diameter of the old one. Since the clearance between the sample and the head part is extremely narrow, it decreases the probability of the sample to interfere with the head part when the sample is rotated. Then a Si_3N_4 membrane window and a pinhole with smaller outer frame were also used.

A new sample stage set was installed. This stage set consists of 3-axis manual stages (X_θ, Y_θ and X) and 3-axis auto stages (θ, X and Z). All auto stages are controlled via drivers by the LabVIEW programming software (National Instruments Co.). By changing a sample holder, 2-D or 3-D observation mode can be switched compatibly.

3. Improvement of environments

For the optical system, both short-term and long-term stabilities are required. The former one means the terms during the one exposure and vibrations of the sample, mainly caused by the airflow, should be especially suppressed. The latter one means the stability during the acquisition of the CT dataset, at least a few hours in our case, and drifts, caused by changes of the temperature, should be suppressed. These problems are mainly caused by the airflow, which comes from the door opening of the experimental hall and from the air conditioners. This environment was improved by building

the housing. This housing covers the whole optical system from upstream of the condenser optics to the CCD camera (see the photo in Fig. 2 (a)) to prevent the airflow from the outside and to ease the change of the temperature. The change of the temperature causes the drifts by thermal expansion of metal components of the optical system so that the changes should be suppressed below 4.7×10^{-3} [°C/min]*. Frames and covers of the housing were not contacted with the optical system not to conduct their vibrations. The thermocouple sensor of type K was used to log the temperature. In Fig. 2 (b), the temperature at the position of the sample with and without the housing were plotted against time. From these results, the thermal fluctuation, which was calculated from the regions indicated by the arrows, was drastically decreased down from 9.1×10^{-3} to 5.3×10^{-4} [°C/min] in the short-term stability. On the other hand, the long-term stability was estimated by comparing the images of the beginning and 3 hours 15 min later and was about 2.5 μm. This was caused by not the thermal fluctuation but rigidity of the system.

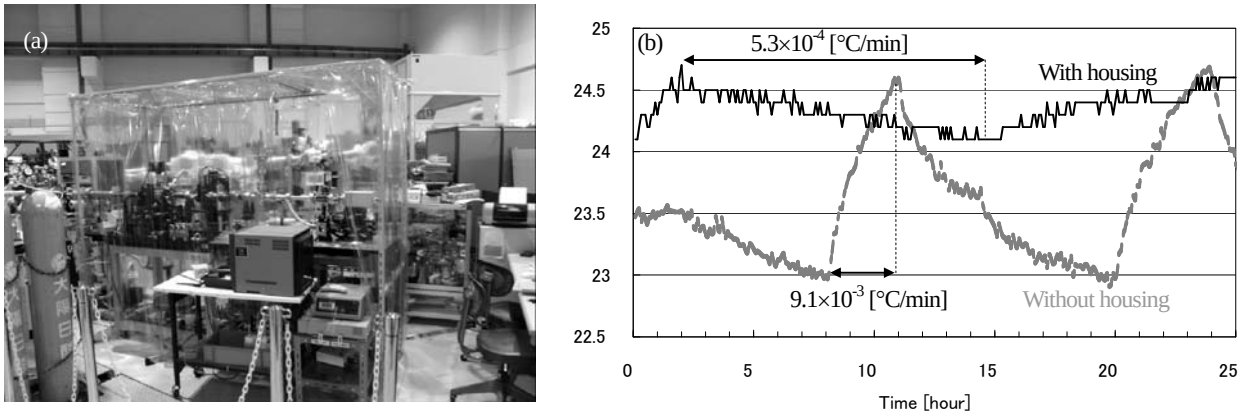

Fig. 2: (a) Housing for the optical system at the BL-12, (b) logs of the temperature at the sample position with/without the housing

4. Processing and Reconstruction

One data set of the CT consists of the projection images of the sample, an I_0 images (i.e. the image without the sample) and a dark image (i.e. the image without x-ray radiation). As preprocessing of the reconstruction, the dark image was subtracted from all the other images as background. The I_0 images were processed by using median filter (radius of 2.0) twice and Gaussian blur filter (radius of 2.00) in order to reduce *salt and pepper* noise caused by lack of statistics. These filtering processes were done by using ImageJ software [9].

---

*: this value was estimated from the thermal expansion of the iron, 11.8×10^{-6} (at 293 K) [8], and the spatial resolution of 55 nm at the diffraction limit with assuming that the height of the optical table was 1.0 m, the direction of the thermal expansion is vertical only and the exposure time is 1 min.

Since acquisition of the CT data set takes long time, ring current of the storage ring decreased to ~60%. Then, the intensities of the images were normalized by the ring current. The rotational axes of the projection images were aligned manually with using structural features of the sample as a reference. The cross-sectional images were reconstructed as a 16-bit tiff image by filtered backprojection algorithm [10]. 3-dimensional image data was obtained by stacking the reconstructed cross-sectional images along z-axis.

For volume rendering visualization and analysis, VGStudio MAX 2.0 (Nihon Visual Science inc.) software was used.

5. Results and Discussion

As a test sample, an extended glass capillary tube with polystyrene spheres (ϕ: 1.05 μm) are observed with using the x-ray wavelength of 2.3 nm. The magnification of the image was 1200. Then the voxel size was 40^3 nm^3 and the reconstructed area was $1.0\times1.0\times9.0$ μm^3. The 50 projection images of 180 s exposure were acquired with rotating 3.6 degree each. Top view and overhead view of the 3-dimensional volume rendering images are shown in Figs. 3 (a) and (b) respectively. The cross-sectional image whose position is indicated by an arrow in (b) is shown in Fig. 3 (a). Noticing one of four polystyrene spheres in the projection images (shown in Fig. 4 (a)), accuracy of the rotational axis is evaluated by plotting the orbit of its center in Fig. 4 (b). The rotational axis of the sample is horizontal direction in Fig. 4 (b). Ideally, these plots draw vertical straight line (ideally, or only one point). This staggering path was mainly caused by wobbling of the rotational stage and drift of the sample stages.

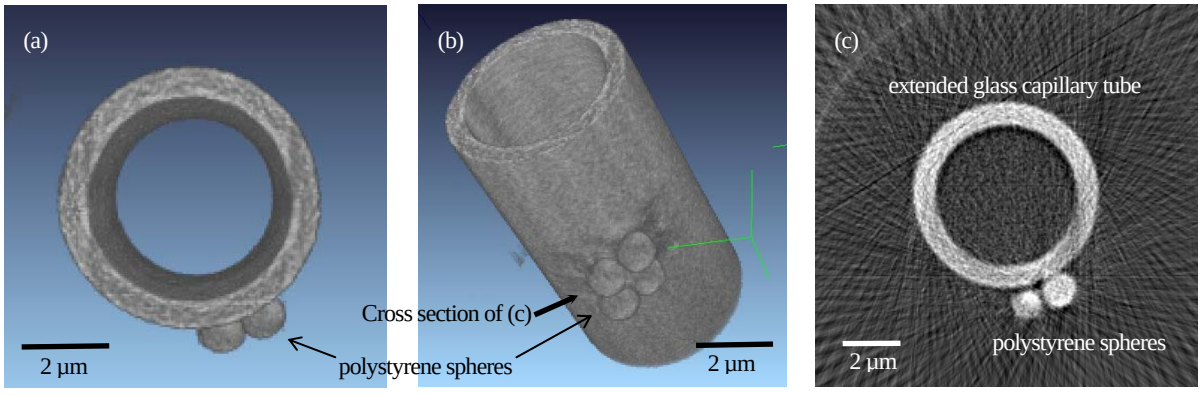

Fig. 3: 3-dimensional images of the extended glass capillary tube and polystyrene spheres from (a) top view and (b) overhead view. (c) A Cross sectional image indicated in (b).

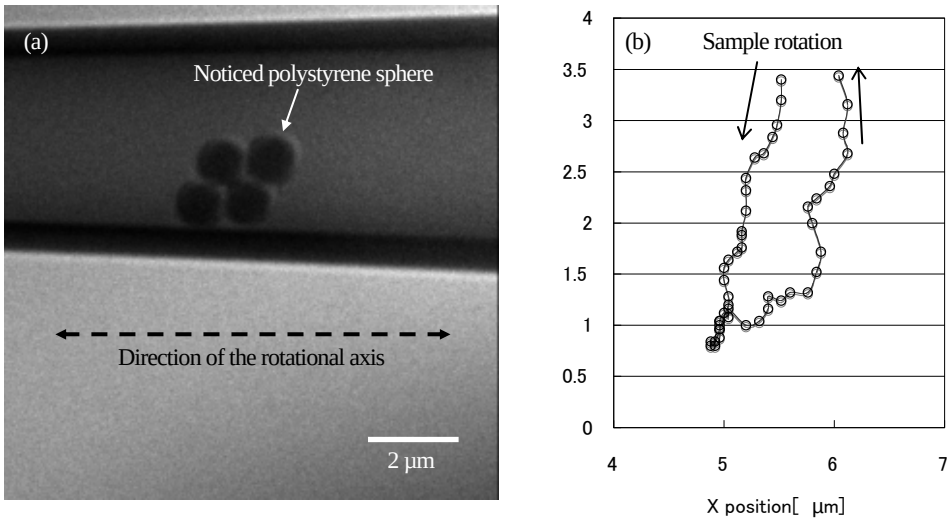

Fig. 4: (a) example of the projection image of the test sample.
(b) Orbit of the center of the one polystyrene sphere is plotted.

As an application, iron bacterium (species was not identified) was observed with using x-ray wavelength of 1.9 nm. The iron bacterium was set on the tip of the extended glass capillary tube and was dried. The magnification of the image was 1000. Then the voxel size was 48^3 nm^3 and the reconstructed area was 12×12×11 μm^3. The 50 projection images of 150 s exposures were acquired with rotating 3.6 degree each. The volume rendering image is shown in Fig. 5 (a). The whole bacterium was covered with sludge. Its cross sectional images whose positions are indicated by arrows in (a) are shown in Figs. (b) and (c). From the cross sectional images, shell like structures were seen but obvious contrast was not obtained.

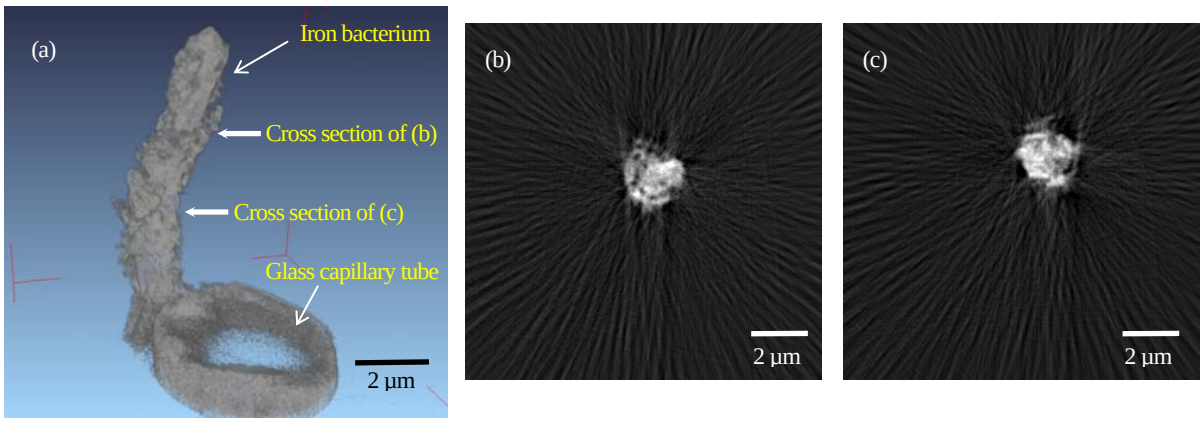

Fig. 5: (a) 3-dimensional volume rendering image of the iron bacterium and (b), (c) its cross sectional images indicated by arrows in (a)

6. Summary

In this study, the CT system for the SXRM was constructed and some samples were observed 3-dimensionally. However, the living samples, such as cells, bacteria and plankton, have not been observed yet. In the case of observation of the living sample by the CT, radiation damage from x-ray is critical so that a cryo-cooling of the sample must be needed [11]. The present cryo-cooling system of BL-12 was designed for 2-dimensional imaging only and was not available for performing the CT (i.e. not suitable for using the rotational stage) [12]. The new cryo-cooling system for the CT, including a thermal insulation housing, circuit and control software, is under development.

A new objective FZP (ATN/FZP-S38/84, NTT-AT N) is due to be installed. This FZP has outermost zone width of 38 nm, ~18% larger N.A. and 27% longer focal length than the objective FZP in this study. These changes of the optical properties enable for performing the CT. The installation the new objective FZP will achieve the spatial resolution of 46 nm theoretically and will enable brighter optics.

References

[1] D. Weiß, G. Schneider, B. Niemann, P. Guttmann, D. Rudolph and G. Schmahl, *Ultramcroscopy*, **84**, (2000), 185-197.

[2] C. A. Larabell and M. A. Le Gros, *Molecular Biology of the Cell*, **15**, (2004), 957-962.

[3] M. Hoshino and S. Aoki, *Applied Physics Express*, **1**, (2008), 067005.

[4] M. Beertilson, O. v. Hofsten, U. Vogt, A. Holmberg and H. M. Hertz, *Optics Express*, **17**, (2009), 11057-11065.

[5] A. Hirai, K. Takemoto, K. Nishino, N. Watanabe, E. Anderson, D. Attwood, D. Kern, M. Hettwer, D. Rudolph, S. Aoki, Y. Nakayama and H. Kihara, *J. Synchrotron Rad.*, **5**, (1998), 1102-1104.

[6] A. Hirai, K. Takemoto, K. Nishino, B. Niemann, M. Hettwer, D. Rudolph, E. Anderson, D. Attwood, D. P. Kern, Y. Nakayama and H. Kihara, *Jpn. J. Appl. Phys.*, **38**, (1999), 274-278.

[7] B. Niemann, D. Rudolph and G. Schmahl, *Opt. Commun.*, **12**, (1974), 160.

[8] National Astronomical Observatory (ed.), *Chronological Scientific Tables*, Maruzen, (2003), pp. 399.

[9] http://rsb.info.nih.gov/ij/

[10] A. C. Kak and M. Slaney, *Principles of Computerized Tomographic Imaging*, IEEE Press, (1988), pp. 60-68.

[11] G. Schneider, E. Anderson, S. Vogt, C. Knöchel, D. Weiss, M. Legros and C. Larabell, *Surf. Rev. Lett.*, **9**, (2002), 177-183.

[12] Kimura, K. Takemoto and H. Kihara, *Jpn. J. Appl. Phys.*, (2010), submitted.